A STUDY OF

THE EFFECT OF ADHESIVE AND MATRIX STIFFNESSES

ON THE AXIAL, NORMAL, AND SHEAR STRESS DISTRIBUTIONS

OF A BORON-EPOXY REINFORCED COMPOSITE JOINT

By

William Edward Howell

B.S. June 1962, North Carolina State University

A Thesis submitted to

The Faculty of

The School of Engineering and Applied Science

of The George Washington University in partial satisfaction

of the requirements for the degree of Master of Science

December 1974

Thesis directed by

Dr. Herbert A. Leybold

Assistant Professorial Lecturer

ABSTRACT

A finite element model of a composite, bonded, step joint was developed. The bonded joint model consisted of two straps of titanium with four steps each, one ply of boron-epoxy bonded to each step, adhesively bonded in a symmetrical manner. A titanium face sheet was bonded to each strap to complete the structural model. The joint design was hypothetical and not intended to represent any specific structural joint. It was developed as a versatile tool for performing parametric studies to determine the effects of various materials properties and joint geometries on the stresses in a bonded step joint. Using this model and the NASTRAN computer program, an analytical investigation of the effect of matrix and adhesive stiffnesses on the axial and shear stresses of the joint was conducted. There was no appreciable change in the stresses due to changes in the stiffness of the adhesive which was varied from 345 MPa to 3100 MPa. However, increasing the modulus of the matrix from 1380 MPa to 6900 MPa caused a 12 percent increase in the boron fiber axial stress. The analysis demonstrates that the finite element model is a viable tool for making detailed analyses of the stresses in a step joint with an imposed load. It can be of significant value in the design of more efficient (higher strength to weight) joints tailored to specific applications.

ACKNOWLEDGMENTS

The author is indebted to the National Aeronautics and Space Administration for the sponsorship of this investigation. Acknowledgment must also be given to Donald J. Baker of AARL-Langley Research Center for his assistance in the operation of the NASTRAN computer program and in generating the contour plots used in this thesis. The author wishes to extend his appreciation to Dr. Herbert A. Leybold of NASA-Langley Research Center for his guidance and encouragement in the preparation of this thesis. Gratitude must also be extended to Richard A. Pride of NASA-Langley Research Center for his guidance in the study of metal-composite bonded joints.

TABLE OF CONTENTS

LIST OF TABLES

LIST OF FIGURES

Page

LIST OF SYMBOLS

Calculations were made in U.S. Customary Units. All values were converted to and are given in the International System of Units (SI).

X ' cartesian coordinate in axial direction of boron fibers

Y cartesian coordinate normal to the direction of boron fibers

σ axial stress

τ shear stress

Subscript

max maximum value

CHAPTER I

INTRODUCTION

Beginning with the earliest flying machines, aircraft designers and builders have continually battled the problem of structural weight. One approach used to develop more efficient structures is high modulus fibers or cloth in a plastic matrix. The earliest attempt to apply this technique to aircraft structures is recorded in the patent application by Robert Kemp in 1916 (ref. 1). However, it was not until 1944 that the first aircraft flew with a structural component (the aft fuselage) which was fabricated using this technique. The material used for the structure was fiberglass cloth in a plastic matrix. Materials of this type are normally referred to as composites. Today a number of other composite materials, such as graphite and boron in a plastic matrix, have been developed; however, there has been very little use of these composite materials in aircraft structures. A major reason why these materials have not been used more frequently is the lack of confidence in composite structures.

Aircraft designers are continuing to develop more efficient structures and to make the best use of the high modulus composite materials. In recent years considerable effort has been expended toward this end. Reference 2

describes a number of existing research programs designed to demonstrate the feasibility of composite structures. In the use of these composites, whether for entire structural components or for selective reinforcement of metallic structures, almost all applications have structural attachments consisting of metallic fittings or concentrated load points. Developing an efficient design for the transition from composite to metal has been one of the major problem areas encountered in the use of composites. To solve this problem, a number of different bonding techniques such as lap shear, scarf, and step joints have been proposed (refs. 3 through 11). Figure 1 is an example of how these techniques can be applied to practical situations. Composite structures such as this one are first attempts at designing and fabricating aircraft primary structures. With appropriate study considerable refinement of such structures is possible. In order to accomplish this, knowledge of the influence of the various material properties and joint geometries is needed. Therefore, in the design of bonded joints, an understanding of the stresses and strains induced in the joints by applied loads is needed in order to develop the most efficient structures.

The purpose of this thesis is to develop a finite element model of a bonded step joint and to present the analytical results of a stress analysis of the joint. The

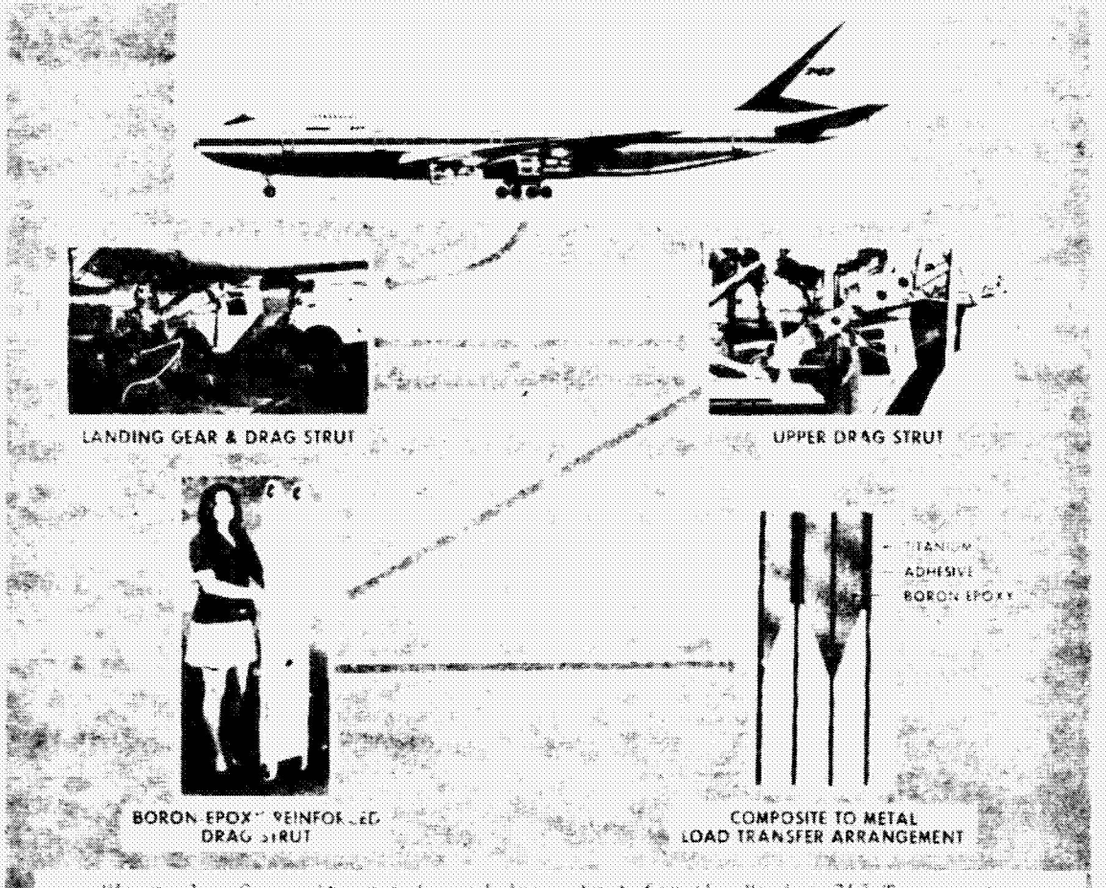

Figure 1.- Composite reinforced drag strut for the Boeing 747 Transport.

model developed was a symmetrical, eight-step, titanium-boron-epoxy joint and represents a general type of bonded step joint with which numerous parametric studies can be made. Such studies will be helpful in the development of more efficient bonded joints designed and tailored to specific applications. Using the finite element model of the step joint a study of the effect of adhesive and matrix stiffnesses on the axial, normal, and shear stress distributions in the joint was made and is included as a part of this thesis. The bonded joint analyzed is hypothetical but is representative of structural joints that are being experimentally evaluated for aerospace applications. For example, the joint model developed for this thesis could be used to approximate the stresses and strains induced in the joints of the structure shown in fig. 1. The NASA Structural Analysis Program NASTRAN (ref. 12) was used for the analysis. The elastic modulus of the adhesive was varied from 345 MPa to 3100 MPa with the nominal value of a commonly used adhesive of 1030 MPa. The elastic modulus of the composite matrix material was varied from 1380 MPa to 6900 MPa with a nominal value of 3100 MPa. These nominal values were used to analyze the axial, normal, and shear stresses in the joint; then, the elastic moduli were varied to determine their effect on the stresses in the joint.

CHAPTER II

BONDED STEP JOINT

The bonded step joint developed for and analyzed in this thesis was that of a symmetric eight-step joint (fig. 2). Each of the four-step titanium straps had one ply of boron-epoxy bonded to each step. The epoxy matrix material was used to adhesively bond the boron-epoxy to the titanium straps. These two straps and the associated composite material were bonded together with an adhesive. A titanium face sheet was also bonded to each strap to complete the joint structure. The finite element model was extended sufficiently far beyond each end of the joint to preclude any influence of edge effects in the joint.

This geometry was chosen for several reasons: it represents a typical step joint in bonded, composite joints; it approximates scarf joints; tensile test specimens of the configuration can be readily fabricated; and the finite element model of the joint has relatively few degrees of freedom which helps keep the computer cost down. Four steps were chosen for each strap of titanium in order to keep the model small and because it was assumed to be sufficient since the significant peak stresses were expected to occur in the first three steps (refs. 10 and 13).

Figure 2.- Eight-step, bonded, titanium-boron-epoxy, symmetrical joint.

CHAPTER III

FINITE ELEMENT MODEL

The finite element model developed to study the bonded step joint consists of quadrilateral elements. Since the joint is symmetrical, it is necessary to model only one-half of it. Figure 3 is a sketch of the analytical model showing the elements and constituent arrangement. This sketch is not drawn to scale; it is presented only to show the elements and the relative arrangement of the four materials (i.e., titanium, adhesive, epoxy matrix, and boron fibers) in the model. The model was arranged so that the material properties of each constituent could readily be changed. In order to study the stresses in each constituent of the composite, each ply of boron-epoxy was divided into equal volumes of boron and epoxy. This is the nominal volume fraction normally used for boron-epoxy (ref. 14). For this model the boron filament volume was assumed to be distributed in a continuous, uniformly thick layer of boron sandwiched between equal volumes of epoxy. In order to simulate the epoxy bond in an actual composite layup, the end of each boron fiber was bonded to the titanium strap with an element of epoxy. Although this bond thickness, 0.25 cm, is larger than those normally fabricated in composite structures (thicknesses up to approximately 0.15 cm), it was not

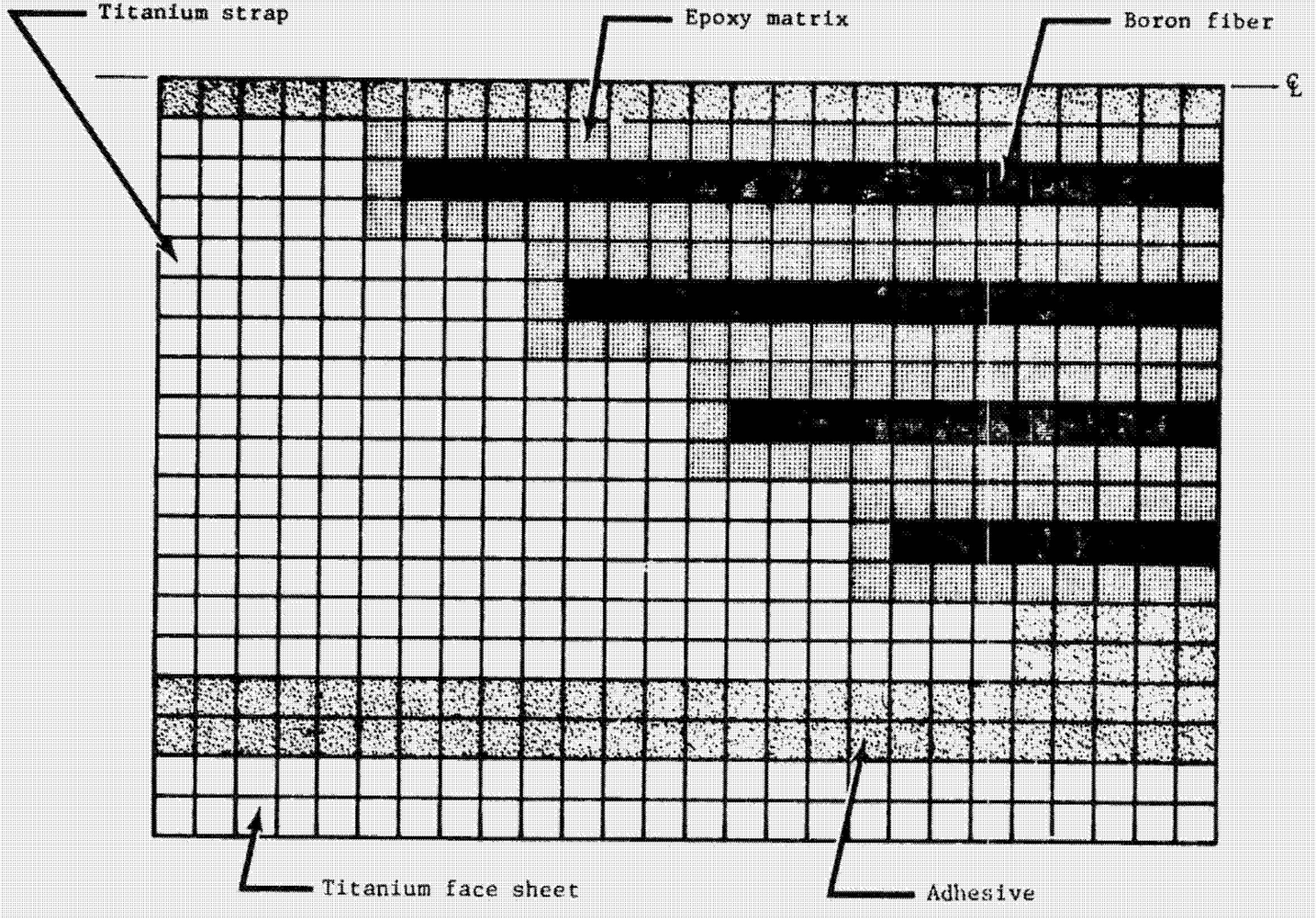

Figure 3.- Finite element model of one-half of bonded joint.

considered to significantly effect the results.

The elements and grid points were numbered from left to right starting at the lower left corner of the model. The model has 540 grid points, 494 elements, and 1033 degrees of freedom. These degrees of freedom consist of translational motion in the x and y directions for all grid points except those at x=0 and those at $y=y_{max}$ (fig. 4). Figure 4 is a sketch of one-half of the joint showing the imposed boundary conditions. The neutral axis of the joint is the upper horizontal line and is marked centerline. The grid points at x=0 are restricted to translational motion in the y-direction. This fixes the left end of the model to allow the right end to be displaced and allows displacement in the y-direction to account for the Poisson effect. Those points at $y=y_{max}$ are restricted to translational motion in the x-direction since they are at the neutral axis of the model. In axial loading the neutral axis would not be displaced until instabilities were achieved. This study does not include such deformations. The grid point at x=0 and $y=y_{max}$ is restricted in both directions since it is at the neutral axis and at the fixed, left end of the model.

Since it would be extremely difficult to determine the load values for each grid point, at the right end of the model, a uniform displacement (~~0.030~~ 0.032 cm) was imposed on all the grid points at the right end of the model as shown by

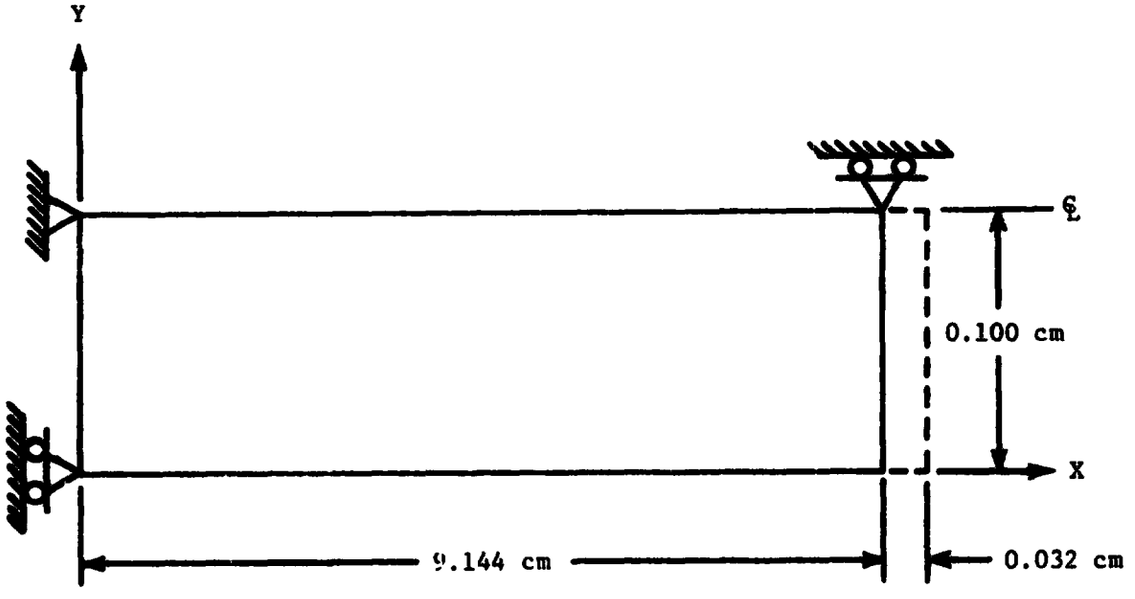

Figure 4. - Boundary conditions imposed on the finite element model.

the dashed line in fig. 4. The uniform displacement simulated an axial load on the model and was calculated from strain measurements published in ref. 13.

The assumptions made for this analysis were:

1. Stress-strain relationship is linear within the area of interest for both the epoxy matrix and adhesive.
2. Poisson's ratio of epoxy equals 0.3
3. Poisson's ratio of adhesive equals 0.4
4. Elastic modulus of titanium equals 1.10×10^5 MPa
5. Elastic modulus of boron equals 3.45×10^5 MPa
6. Plane stress (Membrane elements were used in the NASTRAN program.)

The NASTRAN computer program is a finite element program developed under NASA contract. It was developed as an aid in the analysis and design of general structures. The program computes the axial, normal, and shear stresses of the elements; the grid point displacements; and the forces at the constrained grid points. Only the stresses will be presented in this analysis.

CHAPTER IV

RESULTS AND DISCUSSION

The numerical results presented in this thesis are believed to be within 6 percent of what they would be if the joint were loaded experimentally. Creditability of this statement is based on the results presented in ref. 13 where analytically determined strains compared favorably with measured strains in the bonded joint. The numerical analysis techniques of ref. 13 and this thesis are identical. A different finite element model was developed for each joint. However the differences in the models are not expected to significantly affect the accuracy of the results.

Nominal values of 3100 MPa and 1030 MPa were used respectively for the elastic moduli of the epoxy matrix and adhesive systems. These values represent those of commonly used systems and were used as a base for the stress analysis. Before discussing the effects of changes in these moduli on the axial and shear stress distributions in the joint, the stresses developed using the nominal moduli values will be discussed.

A contour plot of the axial stress distribution in the joint model is shown in fig. 5. A discussion of how such contour plots are generated by the use of a digital computer program is given in ref. 15. The contour lines are at 69 MPa

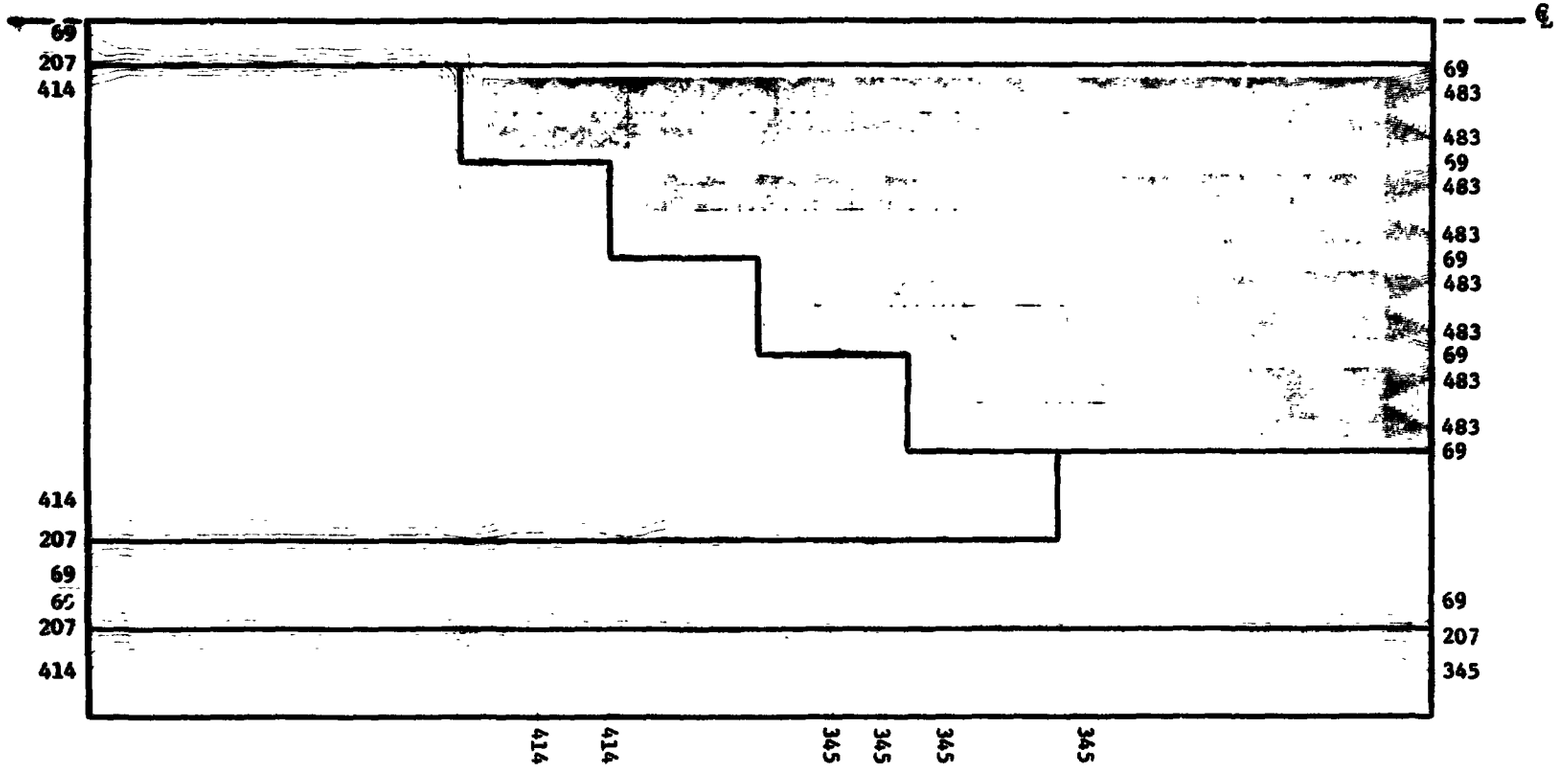

Figure 5. - Contour plot showing the axial stress distribution in the joint model. (Contour lines are at 69 MPa intervals.)

intervals. Dark lines have been added to the plot to show the step joint and the various constituents of the model. The boron fibers are readily identified by the four concentrations of contour lines, indicating the areas with the highest axial stresses. The peak stress occurs in the boron fiber adjacent to the centerline of the model. This peak stress occurs just above the matrix bond at the start of the next step. Perturbations in the axial stress in the first boron fiber also occur at each of the other two step locations and at the end of the titanium strap. These perturbations will be discussed in greater detail later in this thesis. Likewise, each change in configuration causes perturbations in the stress distribution of each of the other fibers. This is also true for the titanium strap and face sheet. No appreciable axial stresses are developed in the adhesive and matrix materials.

A similar contour plot for the normal stress distribution is shown in fig. 6. In this plot the contour lines are at 3.45 MPa intervals. Dark lines have been added to the plot to show the step joint and the various constituents of the model. The peak normal stresses, in both the boron-epoxy and the titanium, are at the same locations as the peak axial stresses in fig. 5 and are related to these latter stresses through the Poisson effect. Note that there is zero normal stress at all edges.

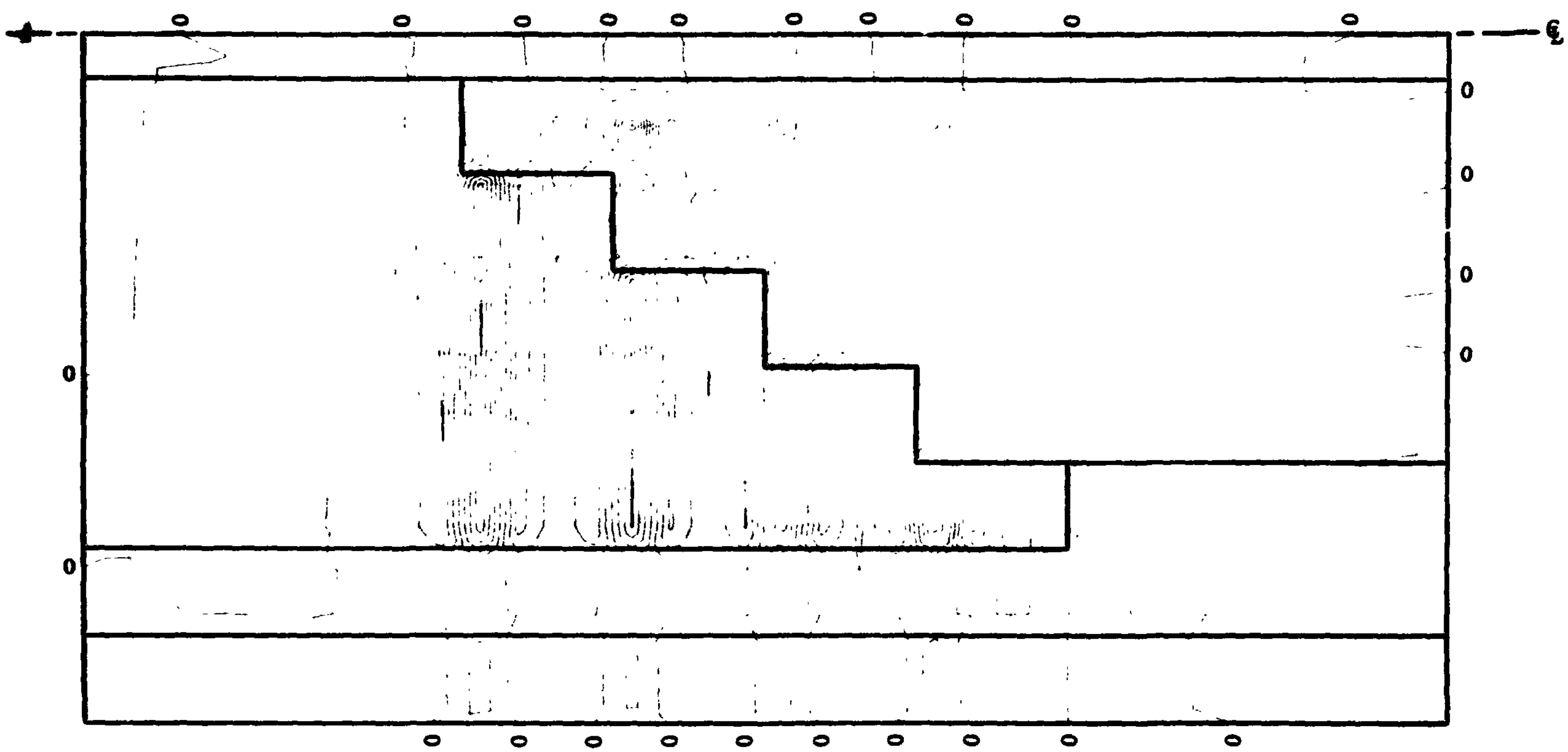

Figure 6. - Contour plot showing the normal stress distribution in the joint model. (Contour lines are at 3.45 MPa intervals.)

Figure 7 is a contour plot of the shear stress distribution in the joint model. The contour lines are at 1.38 MPa intervals. The specific locations of the peak shear stresses are readily identified and are in the immediate vicinity of the bonded step joint. The critical shear stresses occur in the first ply of boron-epoxy and will be discussed in greater detail later in the thesis. There is essentially no shear stress developed in the adhesive layers or in the titanium face sheet.

In order to look at the stresses in critical areas of the joint in greater detail than has been shown in the contour plots, the axial and shear stresses in certain rows of elements are presented. Figure 8 is a plot of the normalized axial stress plotted as a function of distance along the model of the row of elements containing the first ply of boron fibers. This row of elements is specified by the labeled and dotted area in the schematic at the top of fig. 8. Starting at the left end of the joint model, the axial stress is constant (approximately 0.29 times the peak stress) along the model to the first step. At this point the stress decreases, rapidly, to essentially zero. This sudden decrease in the axial stress is due to and occurs in the element of epoxy matrix that bonds the end of the boron fiber to the titanium strap (see fig. 3). The next element in the row is boron and the axial stress at this point (the

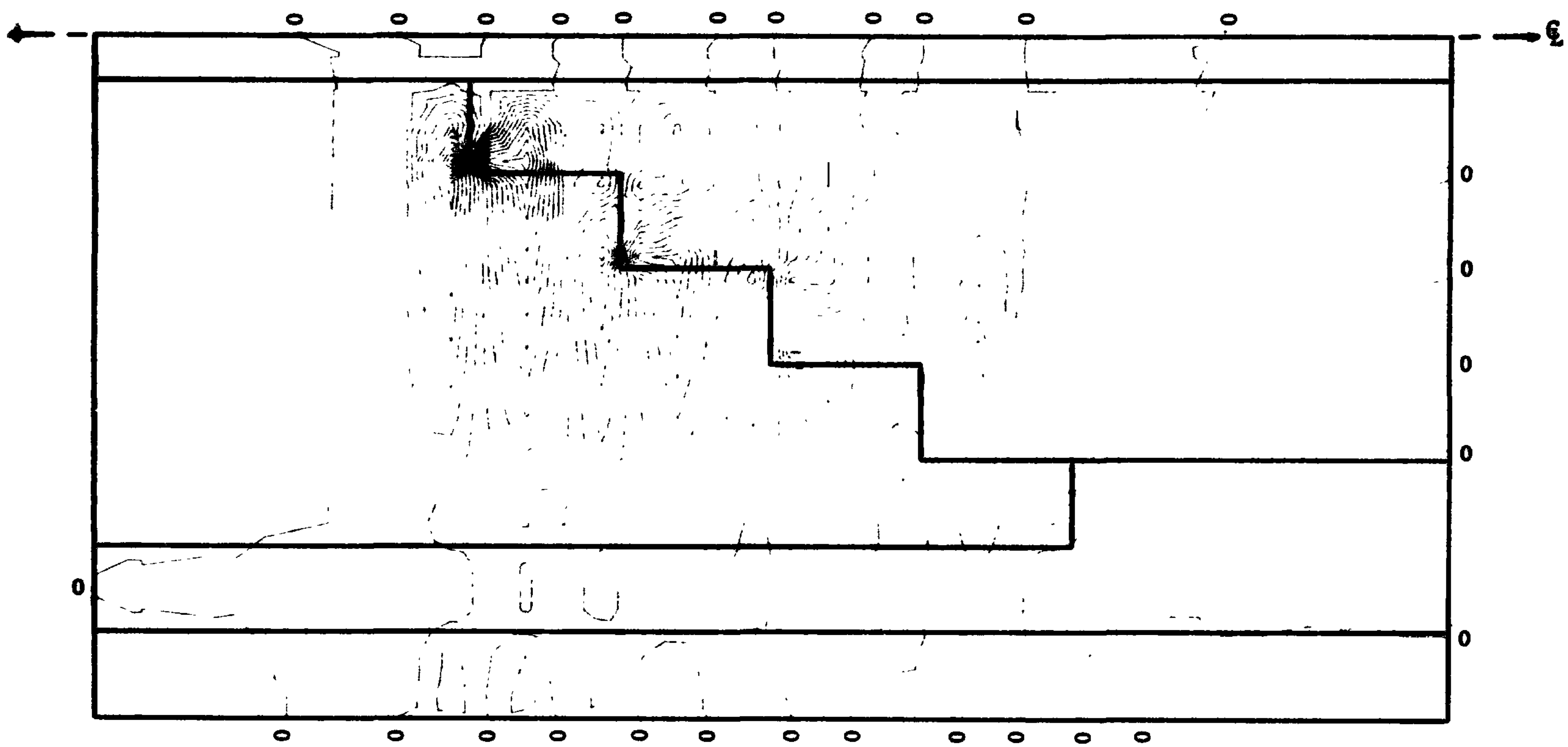

Figure 7. - Contour plot showing the shear stress distribution in the joint model. (Contour lines are at 1.38 MPa intervals.)

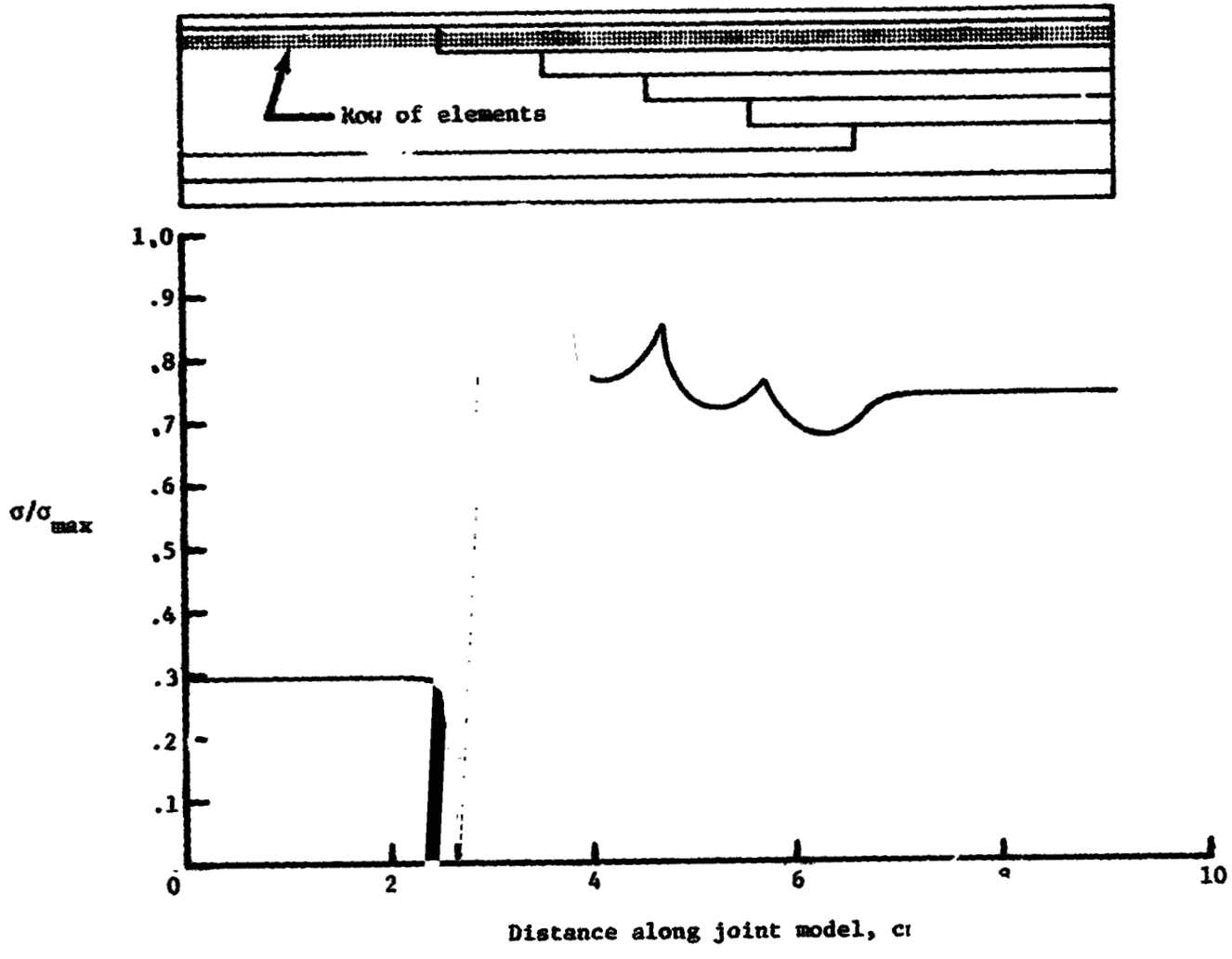

Figure 8. - Axial stress along the row of elements containing the first ply of boron fibers.

centroid of the element) has increased considerably. From this point the stress continues to increase along the length of the first step. At the start of the second step there is another abrupt increase in the axial stress of the fiber. This peak stress is the maximum axial stress in the joint and is caused by the decrease in effective cross-sectional area at the epoxy bond between the titanium strap and the end of the second boron fiber. From this point the stress continually decreases, with progressively decreasing perturbations caused by the successive steps, until the end of the titanium strap is passed. From the end of the strap to the end of the model there are no further changes in configuration and the axial stress is constant (0.74 times the peak stress). Figure 8 readily points out where the maximum stress occurs in the boron fiber and shows the axial stress profile of an individual ply of a bonded step joint.

Since the shear stresses on the boron fibers are small they were not plotted but are presented in Table I. The computed values in the table are for the row of elements containing the first ply of boron. In the table the normalized values and the actual stress values of the shear stress are listed. These actual stress values are derived from the imposed displacement (0.032 cm) previously described. This displacement is representative of the average strain, over the length of the model, for a realistic design ultimate

TABLE I.- Computed shear stress along the row of elements containing the first ply of boron fibers.

Element number	Distance along model, cm	Shear stress, τ, Pa	τ/τ_{max}*
433	0.318	6.21×10^{2}	0.000
434	0.953	1.38×10^{4}	0.001
435	1.588	3.72×10^{4}	0.003
436	2.222	-7.73×10^{4}	0.063
437	2.413	-7.91×10^{6}	0.646
438	2.667	-1.91×10^{5}	0.016
439	2.921	1.22×10^{7}	1.000
440	3.175	3.12×10^{6}	0.255
441	3.429	4.31×10^{6}	0.352
442	3.683	-1.41×10^{6}	0.115
443	3.937	4.42×10^{6}	0.361
444	4.191	9.20×10^{5}	0.075
445	4.445	1.58×10^{6}	0.129
446	4.699	-6.29×10^{6}	0.051
447	4.953	1.68×10^{6}	0.137
448	5.207	1.87×10^{6}	0.015
449	5.461	-1.02×10^{5}	0.008
450	5.715	-3.04×10^{5}	0.025
451	5.969	-1.67×10^{5}	0.014
452	6.223	1.10×10^{3}	0.000
453	6.477	-3.09×10^{5}	0.025
454	6.731	4.06×10^{5}	0.033
455	7.049	5.54×10^{5}	0.045
456	7.557	-5.65×10^{4}	0.005
457	8.192	-2.18×10^{4}	0.002
458	8.827	-1.24×10^{3}	0.000

*τ_{max} = 12.25 MPa

load.

Since the load is transferred from the titanium strap to the boron fibers through the matrix, the shear loading of the matrix is important. Figure 9 is a plot of the normalized shear stress as a function of distance along the model for the epoxy matrix row of elements. This row of elements is specified by the labeled and dotted area in the schematic at the top of fig. 9. As previously stated, the stresses are computed at the centroid of each element. Starting at the left edge of the model, the shear stress is zero nearly all the way to the first step. Near the first step and in the titanium strap, the stress increases rapidly to a maximum. The stress then decreases somewhat in the first element of epoxy, but peaks again in the second element of epoxy. This second element of epoxy is immediately below the end of the boron fiber and is exposed to the highest shear stress of any of the epoxy matrix. In fact this stress is 0.9 times the peak shear stress in the titanium. The matrix immediately below the end of the fiber is the location at which initial joint failure would be expected to occur. From this point the shear stress continually decreases, with progressively smaller perturbations caused by the successive steps, to the end of the model where the shear stress is zero.

Since the axial stresses in the epoxy matrix are

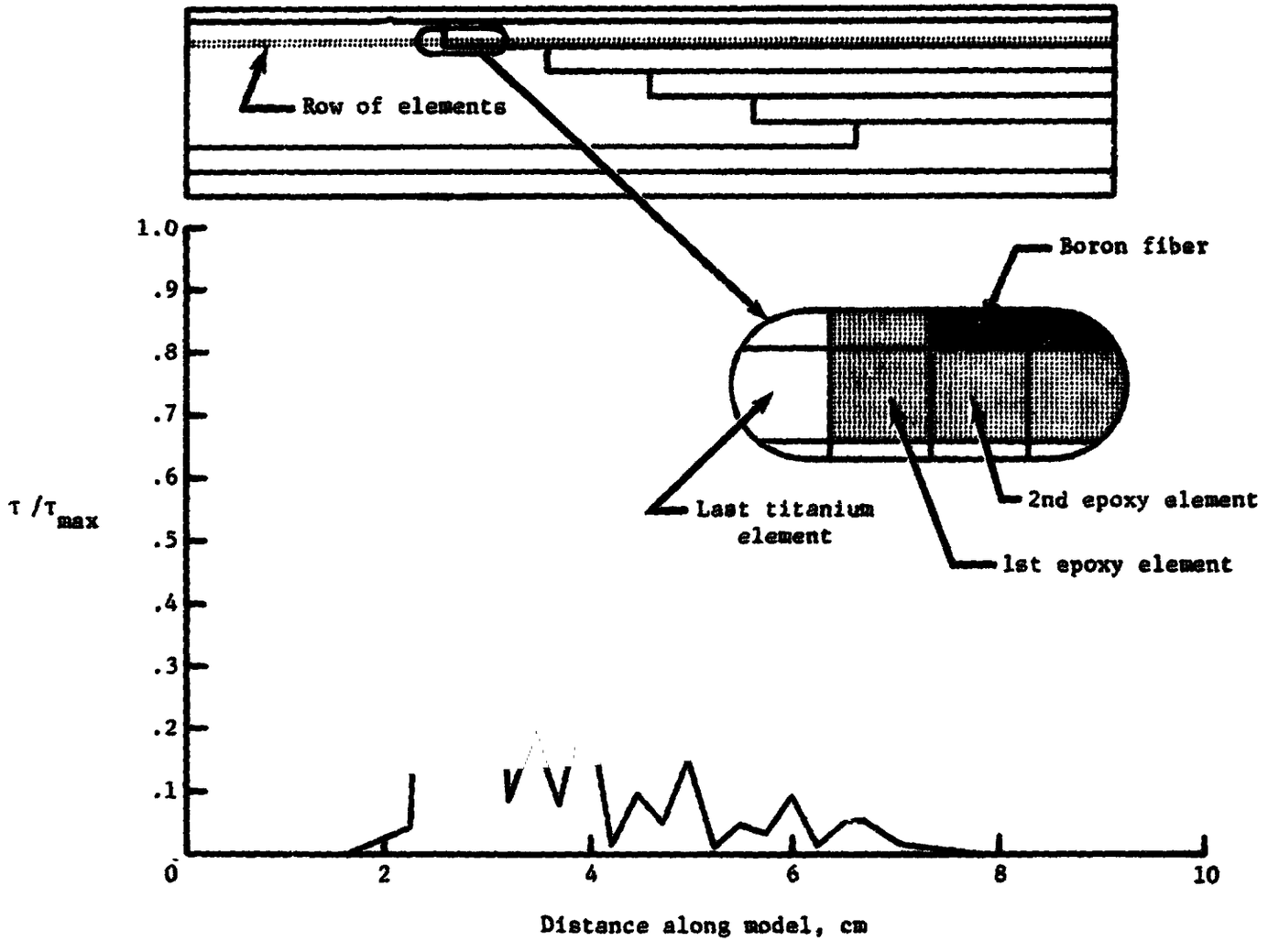

Figure 9. - Shear stress along the row of elements containing epoxy matrix of the first ply of boron-epoxy.

relatively small, they were not plotted but are presented in Table II. Both the normalized and actual values are presented. The actual stress values are derived from the imposed displacement of 0.032 cm.

In the analysis two specific locations were considered; the matrix element exhibiting the highest shear stress (fig. 9) and the element of the boron fiber immediately above the matrix element. Figure 10 presents the axial stress data for the matrix element. The normalized axial stress is plotted as a function of the elastic modulus of the adhesive. The four curves are for the different matrix elastic moduli used in the study. It is clear that there is no significant change in the stress due to changes in the modulus of the adhesive. This is no surprise. The adhesive was only used to bond layers of material together (figs. 2 and 3) and, due to its low modulus value has low loading (figs. 5, 6, and 7). There is a significant change in the axial stress of the matrix due to changes in stiffness though. Figure 11 shows this more clearly than fig. 10 by plotting the normalized axial stress as a function of the elastic modulus of the matrix. The increase in the stress is directly proportional to the increase in the modulus. Even with a two fold increase in the stress from that of the nominal value (3100 MPa) the modulus of the matrix is too small to greatly change the overall loading of the model.

TABLE II.- Computed axial stress along the row of elements containing epoxy matrix of the first ply of boron-epoxy.

Element number	Distance along model, cm	Axial stress, σ, Pa	σ/σ_{max}*
406	0.318	4.31×10^8	1.000
407	0.953	4.31×10^8	1.000
408	1.588	4.31×10^8	1.000
409	2.222	4.31×10^8	0.998
410	2.413	4.27×10^8	0.989
411	2.667	1.57×10^7	0.037
412	2.921	1.05×10^7	0.025
413	3.175	1.12×10^7	0.026
414	3.429	1.10×10^7	0.026
415	3.683	1.34×10^7	0.031
416	3.937	9.94×10^6	0.023
417	4.191	1.02×10^7	0.024
418	4.445	1.03×10^7	0.024
419	4.699	1.14×10^7	0.027
420	4.953	9.65×10^6	0.022
421	5.207	9.43×10^6	0.022
422	5.461	9.61×10^6	0.022
423	5.715	1.02×10^7	0.024
424	5.969	9.14×10^6	0.021
425	6.223	8.76×10^6	0.020
426	6.477	8.96×10^6	0.021
427	6.731	9.58×10^6	0.022
428	7.049	9.78×10^6	0.023
429	7.557	9.77×10^6	0.023
430	8.192	9.76×10^6	0.023
431	8.827	9.76×10^6	0.023

*σ_{max} = 431 MPa

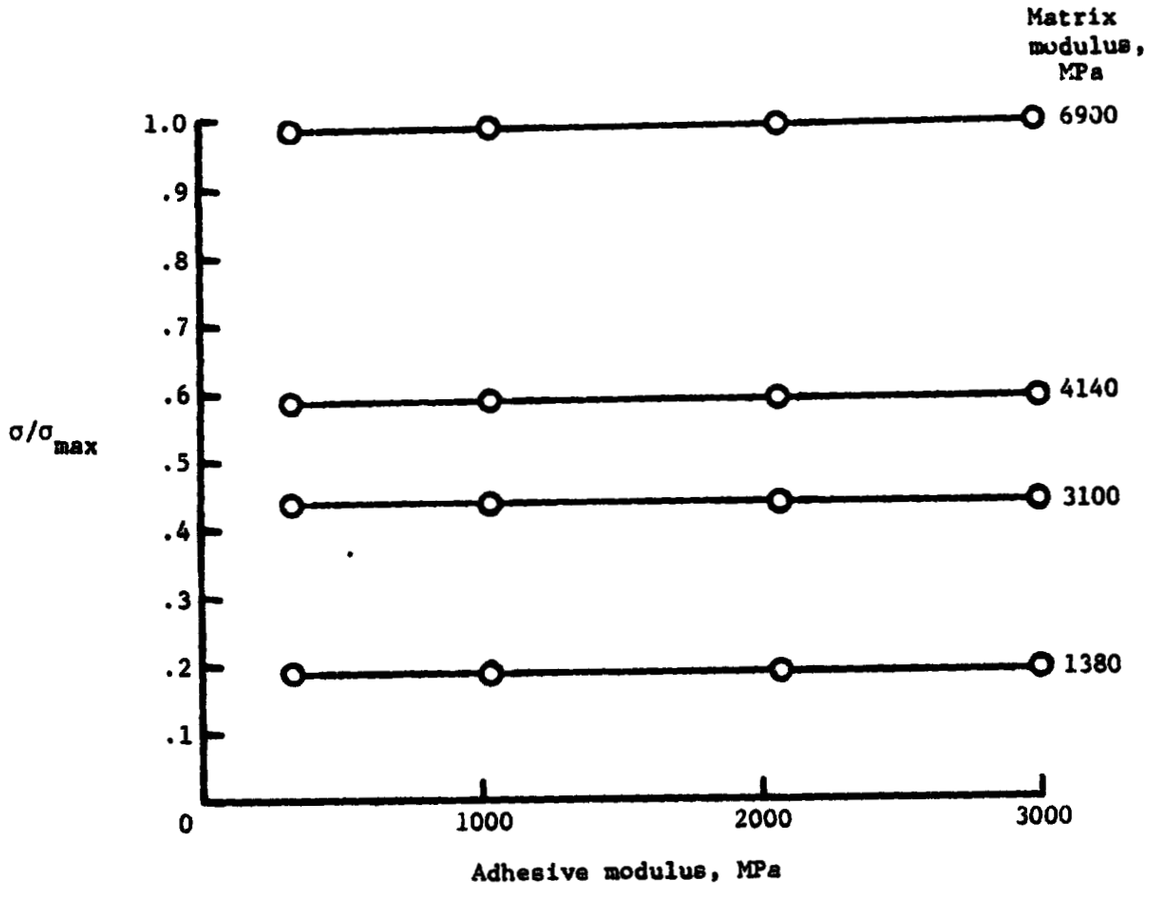

Figure 10. - Effect of matrix and adhesive elastic moduli on the axial stress of the matrix.

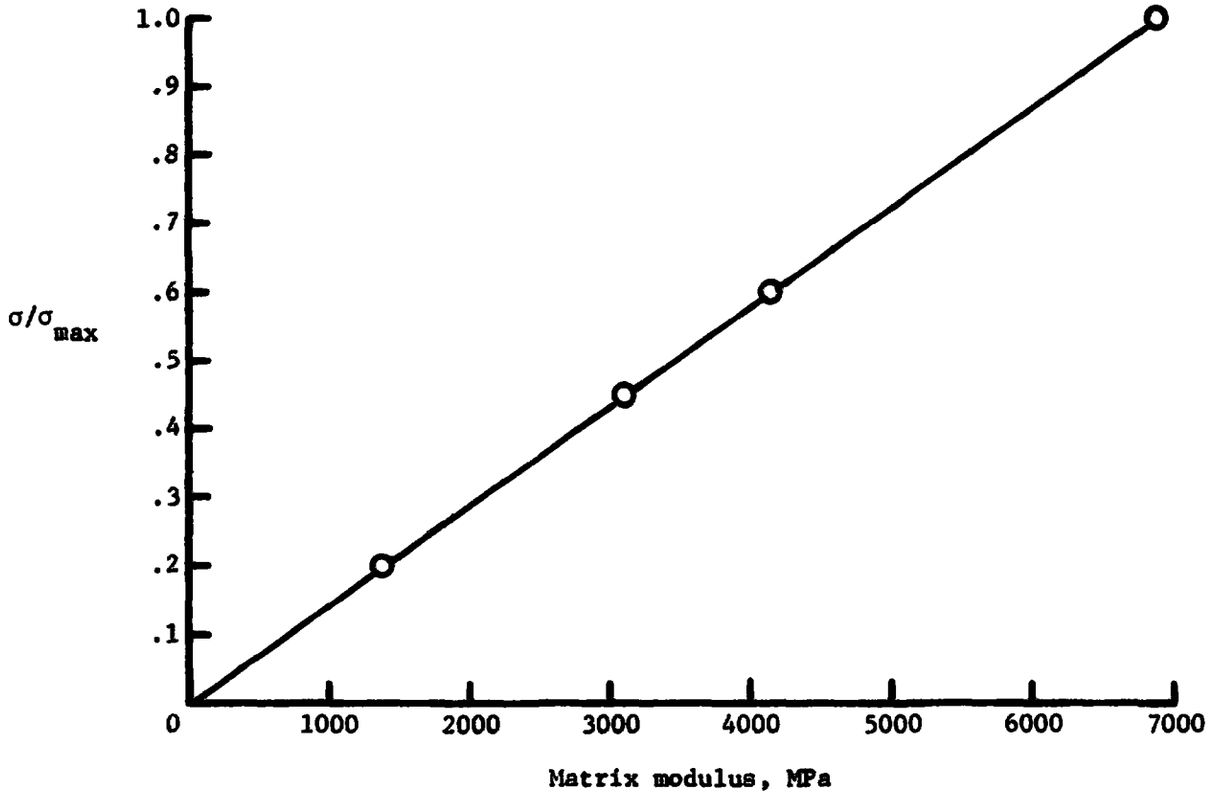

Figure 11. - Effect of matrix elastic modulus on the axial stress of the matrix.

The load is transferred from the titanium strap to the boron fibers by shear deformation of the epoxy matrix. Figure 12 presents the normalized shear stress on the matrix material as a function of the adhesive modulus. The data presented in the figure is for the matrix element exhibiting the highest shear stress (figs. 3 and 9). The envelope indicated by the dotted area represents the total change due to changes in the stiffnesses of the adhesive and matrix. The change in the shear stress due to changing the modulus of the adhesive is insignificant. Although changing the stiffness of the matrix increases the shear stress on the element, the increase is practically insignificant.

Figure 13 shows the normalized axial stress of the boron fiber plotted as a function of the elastic modulus of the adhesive. The portion of the fiber considered is the element directly above the matrix element with the highest shear stress. Again there is no significant change in the stress due to changes in the adhesive modulus. There are changes, however, in the stress due to the changes in the matrix modulus. Figure 14 shows this more clearly than fig. 13 by plotting the normalized axial stress of the boron-fiber element as a function of the elastic matrix modulus. There is a significant change in the axial stress of the fiber element. Increasing the modulus of the matrix from 1380 MPa to 6900 MPa increases the axial stress of the

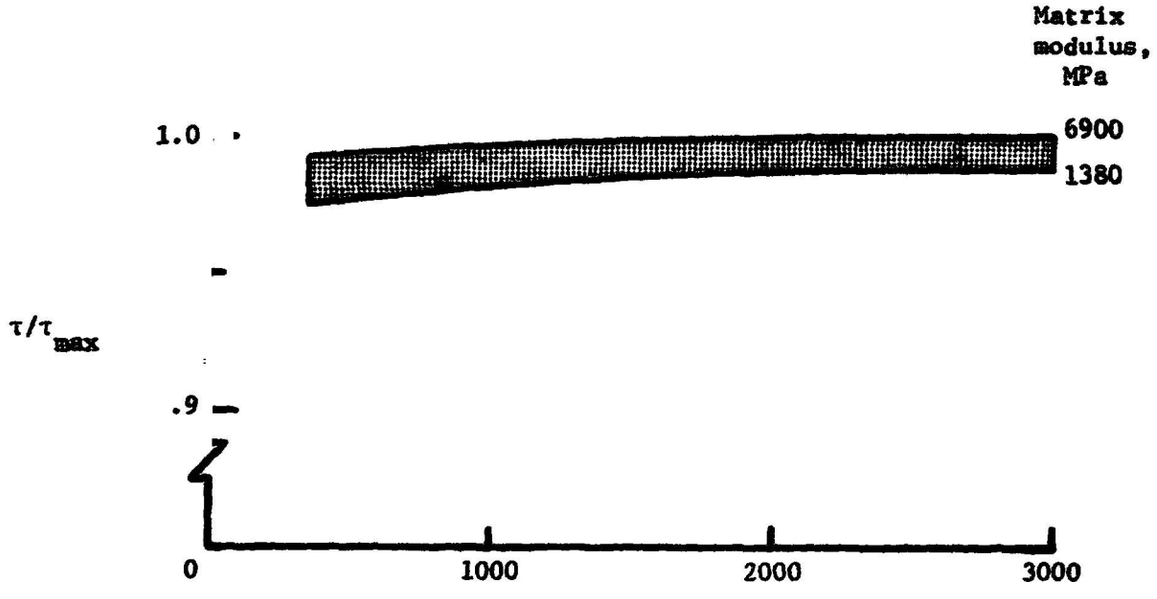

Figure 12. - Effect of matrix and adhesive elastic moduli on the shear stress of the matrix.

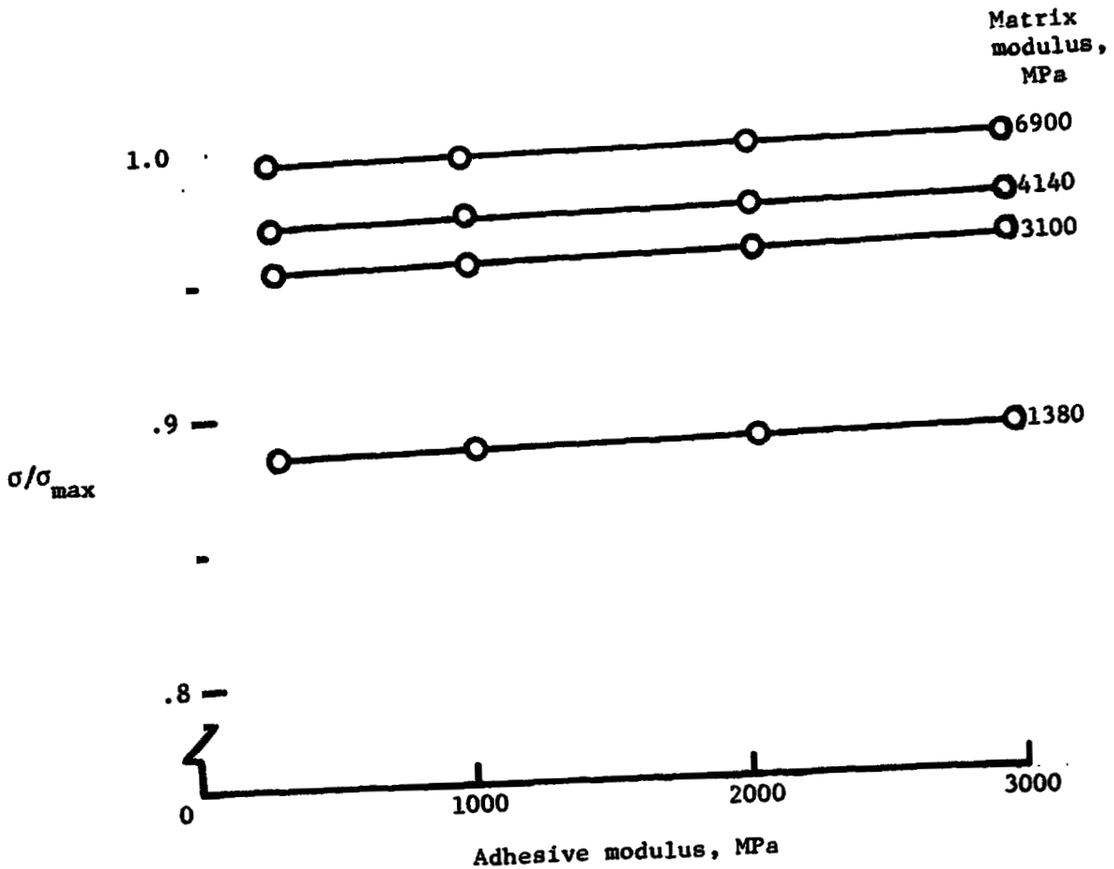

Figure 13. - Effect of matrix and adhesive elastic moduli on the axial stress of the boron fiber.

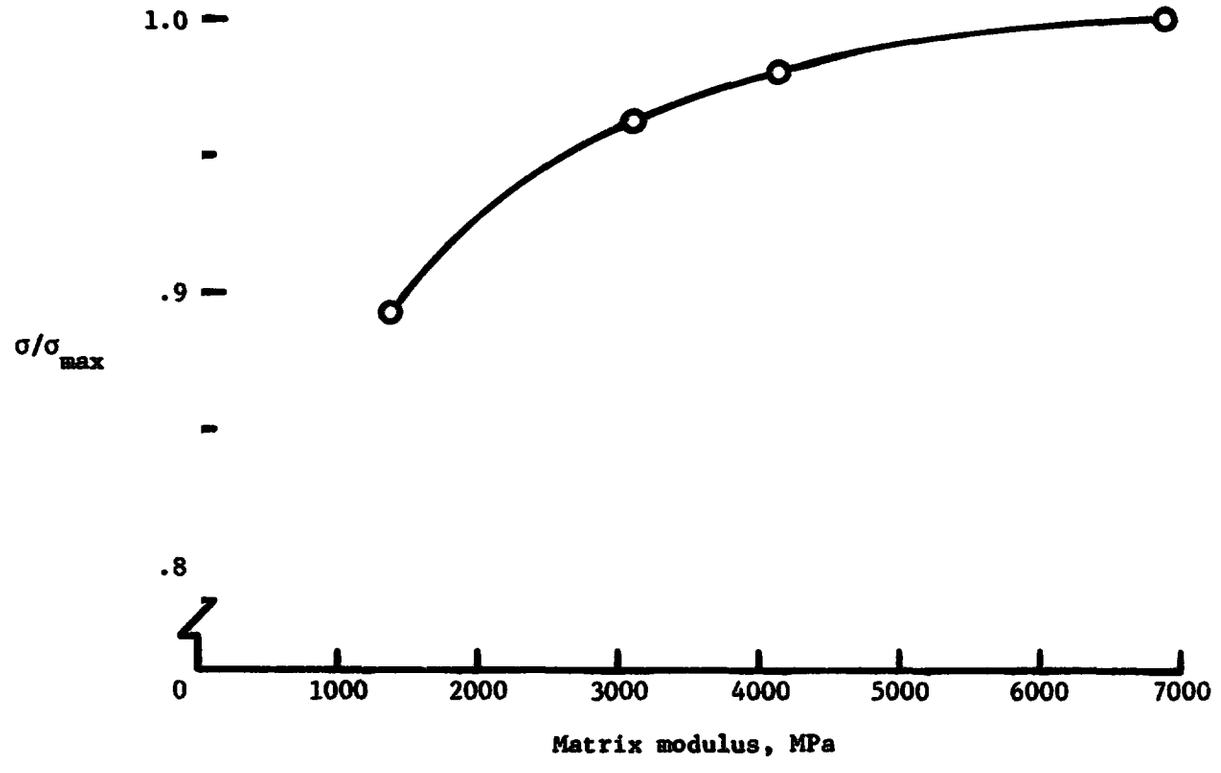

Figure 14. - Effect of matrix elastic modulus on the axial stress of the boron fiber.

fiber element by 12 percent.

The axial stress of the boron fiber is increased by the use of a stiffer matrix. This information can be used as a tool in tailoring joints to specific applications. For example, if the peak shear stress in the matrix is not detrimental, then the incorporation of a stiffer matrix would aid in transferring the load through the joint in a shorter distance and hence would result in a lighter weight structure. Using aluminum as the stiffer matrix would decrease the efficiency of the composite (i.e., the strength to weight ratio would be less with the aluminum than with the polymeric matrix). Therefore a tradeoff between the matrix strffness and composite efficiency is required.

Another way in which the joint model could be used in this type of analysis is to redistribute the load so that it would be transferred more evenly throughout the entire joint. This could be accomplished by the use of a "soft" (low stiffness) matrix material in the first ply and gradually increasing the matrix stiffness in the successive plies.

These are just two examples of the ways in which the finite element model developed in this thesis can be used to aid in the development of more efficient bonded joints or joints tailored to specific applications. The study made using this model is only one of many required in order to

understand the influence of the various parameters (i.e., step length, multiple plies per step, fiber stiffness per ply, and matrix stiffness per ply) and the interactions thereof in bonded composite joints.

CHAPTER V

CONCLUDING REMARKS

A finite element model of a bonded, step joint was developed. The joint design was hypothetical and not intended to represent any specific structural joint but was developed as a versatile tool for performing studies to determine the effects of various material properties and joint geometries on the stresses in a loaded step joint. In this thesis only the moduli of the adhesive and the matrix material were varied in order to determine the effect, if any, of each on the stresses in the bonded joint. It was shown that the stiffness of the adhesive as used in the model had essentially no effect on stresses.

Stiffness of the matrix material, which was also used as the adhesive between the titanium and the boron-epoxy, did effect the stresses in the joint. Changing the elastic matrix modulus changed the stresses to some extent. Although the increase in the matrix modulus (by a factor of five) had little effect on the shear stress of the matrix, it did increase the local axial stress of the boron fiber. This indicates that the stiffer matrix transfers the load into the boron fiber more quickly than one with the nominal value of elastic modulus.

The finite element model developed in this thesis, in

conjunction with the NASTRAN computer program, is a viable tool for making detailed analyses of the stresses in an actual step joint with an imposed load. It can be used to determine the effects of each of the variables in the bonded joint on the stress distribution in the joint. Therefore it can be of significant value in the design of more efficient joints tailored to specific applications.

APPENDIX

NASTRAN INPUT/OUTPUT

The NASTRAN computer program is a finite element program and requires a considerable amount of computer storage, a minimum of 140,000 octal locations of core storage. A detailed description of the program is given in ref. 12. The model used in this static analysis was composed of membrane elements. Although the axial, normal, and shear stresses were the only parameters used in this study, other parameters, such as grid point displacement and forces at the constrained grid points, were also computed. A sample of the input element (CQDMEM), grid point (GRID), and the computed stress output data is enclosed in the appendix and is printed in U.S. Customary Units. Listed below is a brief description of the parameters in each of the columns of the input element and grid cards.

Element Cards

Column 1: CQDMEN is the name of the quadrilateral membrane element.

Column 2: The individual element identifier

Column 3: The number that identifies the element material (titanium, boron, etc.)

Columns 4 - 7: The four grid points of the element

Column 8: Material property orientation angle

Grid Cards

Column 1: Grid is the name used to identify the grid point.

Column 2: The individual grid point identifier

Column 3: Identification number of coordinate system in which the location of the grid point is defined

Column 4 - 6: Cartesian x, y, and z coordinate values

Column 7: Blank

Column 8: Grid point constraints

The rows of dots represent areas of omitted data, and the output stress data is felt to be self-explanatory.

INPUT DATA

```
CARD
COUNT      . 1 .. 2 .. 3 .. 4 .. 5 .. 6 .. 7 .. 8 .. 9 .. 10 .
   1-      CQDMEM  1     1     1     2     29    28    .0
   2-      CQDMEM  2     1     2     3     30    29    .0
   3-      CQDMEM  3     1     3     4     31    30    .0
   4-      CQDMEM  4     1     4     5     32    31    .0
   5-      CQDMEM  5     1     5     6     33    32    .0
   6-      CQDMEM  6     1     6     7     34    33    .0
   7-      CQDMEM  7     1     7     8     35    34    .0
   8-      CQDMEM  8     1     8     9     36    35    .0
   9-      CQDMEM  9     1     9     10    37    36    .0
  10-      CQDMEM  10    1     10    11    38    37    .0
  11-      CQDMEM  11    1     11    12    39    38    .0
  12-      CQDMEM  12    1     12    13    40    39    .0
  13-      CQDMEM  13    1     13    14    41    40    .0
  14-      CQDMEM  14    1     14    15    42    41    .0
  15-      CQDMEM  15    1     15    16    43    42    .0
  16-      CQDMEM  16    1     16    17    44    43    .0
  17-      CQDMEM  17    1     17    18    45    44    .0
  18-      CQDMEM  18    1     18    19    46    45    .0
  19-      CQDMEM  19    1     19    20    47    46    .0
  20-      CQDMEM  20    1     20    21    48    47    .0
  21-      CQDMEM  21    1     21    22    49    48    .0
  22-      CQDMEM  22    1     22    23    50    49    .0
  23-      CQDMEM  23    1     23    24    51    50    .0
  24-      CQDMEM  24    1     24    25    52    51    .0
  25-      CQDMEM  25    1     25    26    53    52    .0
  26-      CQDMEM  26    1     26    27    54    53    .0
  27-      CQDMEM  28    1     28    29    56    55    .0
  28-      CQDMEM  29    1     29    30    57    56    .0
  29-      CQDMEM  30    1     30    31    58    57    .0
  30-      CQDMEM  31    1     31    32    59    58    .0
  31-      CQDMEM  32    1     32    33    60    59    .0
  32-      CQDMEM  33    1     33    34    61    60    .0
  33-      CQDMEM  34    1     34    35    62    61    .0
  34-      CQDMEM  35    1     35    36    63    62    .0
  35-      CQDMEM  36    1     36    37    64    63    .0

   .  .  .  .  .  .  .  .  .  .  .  .  .  .  .  .  .  .  .

 491-      CQDMEM  509   2     509   510   537   536   .0
 492-      CQDMEM  510   2     510   511   538   537   .0
 493-      CQDMEM  511   2     511   512   539   538   .0
 494-      CQDMEM  512   2     512   513   540   539   .0
 495-      GRID    1     0     .0000 .0000 .0000       13456
 496-      GRID    2     0     25.0000 .0000 .0000     3456
 497-      GRID    3     0     50.0000 .0000 .0000     3456
 498-      GRID    4     0     75.0000 .0000 .0000     3456
 499-      GRID    5     0     90.0000 .0000 .0000     3456
 500-      GRID    6     0     100.0000.0000 .0000     3456
 501-      GRID    7     0     110.0000.0000 .0000     3456
 502-      GRID    8     0     120.0000.0000 .0000     3456
 503-      GRID    9     0     130.0000.0000 .0000     3456
 504-      GRID    10    0     140.0000.0000 .0000     3456
 505-      GRID    11    0     150.0000.0000 .0000     3456
 506-      GRID    12    0     160.0000.0000 .0000     3456
 507-      GRID    13    0     170.0000.0000 .0000     3456
 508-      GRID    14    0     180.0000.0000 .0000     3456
 509-      GRID    15    0     190.0000.0000 .0000     3456
 510-      GRID    16    0     200.0000.0000 .0000     3456
 511-      GRID    17    0     210.0000.0000 .0000     3456
 512-      GRID    18    0     220.0000.0000 .0000     3456
 513-      GRID    19    0     230.0000.0000 .0000     3456
 514-      GRID    20    0     240.0000.0000 .0000     3456
```

INPUT DATA

```
CARD
COUNT      .  1  ..  2  ..  3  ..  4  ..  5  ..  6  ..  7  ..  8  ..  9  .. 10  .
  515-     GRID      21        0      250.0000.0000    .0000          3456
  516-     GRID      22        0      260.0000.0000    .0000          3456
  517-     GRID      23        0      270.0000.0000    .0000          3456
  518-     GRID      24        0      285.0000.0000    .0000          3456
  519-     GRID      25        0      310.0000.0000    .0000          3456
  520-     GRID      26        0      335.0000.0000    .0000          3456
  521-     GRID      27        0      360.0000.0000    .0000          3456
  522-     GRID      28        0      .0000    .2500   .0000          13456
  523-     GRID      29        0      25.0000  .2500   .0000          3456
  524-     GRID      30        0      50.0000  .2500   .0000          3456
  525-     GRID      31        0      75.0000  .2500   .0000          3456

   .  .  .  .  .  .  .  .  .  .  .  .  .  .  .  .  .  .  .  .  .  .  .  .

 1016-     GRID      522       0      130.00003.9460   .0000          23456
 1017-     GRID      523       0      140.00003.9460   .0000          23456
 1018-     GRID      524       0      150.00003.9460   .0000          23456
 1019-     GRID      525       0      160.00003.9460   .0000          23456
 1020-     GRID      526       0      170.00003.9460   .0000          23456
 1021-     GRID      527       0      180.00003.9460   .0000          23456
 1022-     GRID      528       0      190.00003.9460   .0000          23456
 1023-     GRID      529       0      200.00003.9460   .0000          23456
 1024-     GRID      530       0      210.00003.9460   .0000          23456
 1025-     GRID      531       0      220.00003.9460   .0000          23456
 1026-     GRID      532       0      230.00003.9460   .0000          23456
 1027-     GRID      533       0      240.00003.9460   .0000          23456
 1028-     GRID      534       0      250.00003.9460   .0000          23456
 1029-     GRID      535       0      260.00003.9460   .0000          23456
 1030-     GRID      536       0      270.00003.9460   .0000          23456
 1031-     GRID      537       0      285.00003.9460   .0000          23456
 1032-     GRID      538       0      310.00003.9460   .0000          23456
 1033-     GRID      539       0      335.00003.9460   .0000          23456
 1034-     GRID      540       0      360.00003.9460   .0000          23456
 1035-     MAT1      1         16.+6  6.15+6   .3      1.0     1.0    1.0     1.0    +ABC1
 1036-     +ABC1     1.0+6     1.0+6  1.0+6
 1037-     MAT1      2         1.50+5 5.360+4  .4      1.0     1.0    1.0     1.0    +ABC2
 1038-     +ABC2     1.0+6     1.0+6  1.0+6
 1039-     MAT1      3         4.50+5 1.730+5  .3      1.0     1.0    1.0     1.0    +ABC3
 1040-     +ABC3     1.0+6     1.0+6  1.0+6
 1041-     MAT1      4         50.0+6 20.8+6   .2      1.0     1.0    1.0     1.0    +ABC4
 1042-     +ABC4     1.0+6     1.0+6  1.0+6
 1043-     PUOMEM    1         1      1.0      0.0     2       2      1.0     0.0
 1044-     PUOMEM    3         3      1.0      0.0     4       4      1.0     0.0
 1045-     SPC       20        27     1        1.25    54      1      1.25
 1046-     SPC       21        81     1        1.25    108     1      1.25
 1047-     SPC       22        135    1        1.25    162     1      1.25
 1048-     SPC       23        189    1        1.25    216     1      1.25
 1049-     SPC       24        243    1        1.25    270     1      1.25
 1050-     SPC       25        297    1        1.25    324     1      1.25
 1051-     SPC       26        351    1        1.25    378     1      1.25
 1052-     SPC       27        405    1        1.25    432     1      1.25
 1053-     SPC       28        459    1        1.25    486     1      1.25
 1054-     SPC       29        513    1        1.25    540     1      1.25
 1055-     SPCADD    5         20     21       22      23      24     25      26     +CONT1
 1056-     +CONT1    27        28     29
           ENDDATA
```

OUTPUT DATA

STRESSES IN QUADRILATERAL MEMBRANES

ELEMENT ID.	STRESSES IN ELEMENT COORD SYSTEM NORMAL-X	NORMAL-Y	SHEAR-XY
1	62.575096E+03	-20.948845E-02	15.047620E-02
2	62.576619E+03	-33.273295E-01	25.287961E-01
3	62.613435E+03	-23.585553E+00	-20.101135E-01
4	63.049340E+03	-54.867345E+00	-12.847069E+01
5	64.534796E+03	-98.624613E+00	33.440910E+01
6	67.782331E+03	74.794389E+01	-14.190539E+00
7	61.440339E+03	-28.574195E+01	-31.007094E+01
8	58.889263E+03	-27.416098E+01	12.625100E+01
9	58.751973E+03	-19.635160E+01	22.602662E+01
10	61.251462E+03	62.173106E+01	-22.540605E+00
11	55.727519E+03	-26.233464E+01	-17.644491E+01
12	53.670376E+03	-17.575318E+01	71.580171E+00
13	53.681723E+03	-22.480569E+01	13.062220E+01
14	56.714579E+03	68.551446E+01	-10.231352E+00
15	50.875399E+03	-30.811107E+01	-82.704229E+00
16	49.107581E+03	-17.485945E+01	56.329022E+00
17	49.375798E+03	-29.474948E+01	36.234638E+00
18	53.611488E+03	87.421809E+01	-23.423703E-01
19	46.508008E+03	-40.823519E+01	58.275998E-01
20	44.810110E+03	-16.755160E+01	57.549866E+00
21	45.004882E+03	-41.778484E+01	-10.224747E+01
22	50.546405E+03	43.025536E+01	71.713838E+00
23	50.566049E+03	22.109271E+00	-25.333610E+00
24	50.405892E+03	-60.773582E-01	-30.017684E-01
25	50.365920E+03	-26.337742E-01	-10.424429E-01
26	50.359953E+03	-55.107128E-02	-71.895599E-03
27	62.575089E+03	-23.377274E-02	14.779905E-02
28	62.576767E+03	-32.980976E-01	23.752455E-01
29	62.614028E+03	-22.050570E+00	-46.385067E-01
30	63.037023E+03	-60.103121E+00	-14.553148E+01
31	64.531705E+03	-10.346471E+01	27.422637E+01
32	67.847508E+03	76.599861E+01	25.365100E+00
33	61.425262E+03	-29.095896E+01	-19.418573E+01
34	58.841362E+03	-21.616344E+01	15.942653E+01
35	58.753140E+03	-19.436798E+01	19.236386E+01

• • • • • • • • • • • • • •

494	59.326805E+01	16.742382E+01	77.864144E-02
495	54.347661E+01	14.720522E+00	51.993059E-02
496	61.591665E+01	-46.871848E+00	-67.834122E-02
497	48.331854E+01	-24.806698E+00	-96.802187E-02
498	50.793740E+01	48.480578E+00	26.530445E-02
499	50.754176E+01	19.832932E+00	33.764577E-02
500	54.676597E+01	89.197691E-01	-29.082439E-02
501	46.523692E+01	-17.670736E+00	-61.246383E-02
502	45.395636E+01	-10.145027E+00	87.275705E-03
503	47.211157E+01	20.390091E+00	21.324199E-02
504	50.287600E+01	45.918357E+00	-21.051489E-02
505	43.827601E+01	-17.582475E+00	-49.532898E-02
506	40.494790E+01	-67.044861E+00	-70.501674E-03
507	42.391434E+01	-33.416843E+00	28.746385E-02
508	47.045313E+01	27.595716E+00	32.438877E-02
509	48.059925E+01	27.498955E+00	94.210941E-03
510	47.381751E+01	48.217385E-01	-36.834320E-03
511	47.206241E+01	-77.289702E-03	-78.783710E-04
512	47.207732E+01	-80.146565E-03	-17.002737E-05

REFERENCES

1. Lubin, George (Editor): Handbook of Fiberglass and Advanced Plastics Composites. Van Nostrand Reinhold Company, New York, 1969.

2. June, R. R.; and Kelly, J. B.: Applications of Advanced Composites for Aircraft. SAMPE Journal, Vol. 3, No. 2, January 1972.

3. Lager, John R.; and June, Reid R.: Design, Analysis, Fabrication and Test of a Boron Composite Beam. Journal of Composite Materials, Vol. II, No. 2, April 1968, pp. 128-137.

4. Erdogan, F.; and Ratwani, M.: Stress Distribution in Bonded Joints. Journal of Composite Materials, Vol. 5, July 1971, pp. 378-393.

5. Oken, S.; and June, R. R.: Analytical and Experimental Investigation of Aircraft Metal Structures Reinforced with Filamentary Composites. Phase I - Concept Development and Feasibility. NASA CR-1859, 1971.

6. Corvelli, N.; and Carri, R. L.: Evaluation of a Boron-Epoxy Reinforced Titanium Tubular Truss for Applications to a Space Shuttle Booster Thrust Structure. NASA TN D-6778, 1972.

7. Blichfeldt, R.; and McCarty, J. E.: Analytical and Experimental Investigation of Aircraft Metal Structures Reinforced with Filamentary Composites. Phase II - Structural Fatigue, Thermal Cycling, Creep, and Residual Strength. NASA CR-2039, 1972.

8. Barker, Richard M.; and Hatt, Fritz: Analysis of Bonded Joints in Vehicular Structures. Presented at the AIAA/ASME/SAE 14th Structures, Structural Dynamics, and Materials Conference, Williamsburg, Virginia, March 20-22, 1973.

9. Kelley, J. B.; and June, R. R.: Residual Stress Alleviation of Aircraft Metal Structures Reinforced with Filamentary Composites. NASA CR-112207, 1973.

10. Hart-Smith, L. J.: Analysis and Design of Advanced Composite Bonded Joints. NASA CR-2218, 1973.

11. Renton, W. James; and Vinson, Jack R.: On Fatigue Behavior of Bonded Joints in Composite Material Structures. Presented at the AIAA/ASME/SAE 15th Structures, Structural Dynamics, and Materials Conference, Las Vegas, Nevada, April 17-19, 1974.

12. MacNeal, Richard H. (Editor): The NASTRAN Theoretical Manual (Level 15). NASA SP-221(01), 1972.

13. Howell, William E.: Bonded Composite-To-Metal Scarf Joint Performance in an Aircraft Landing Gear Drag Strut. Paper presented at the Army Symposium on Solid Mechanics, 1974: The Role of Mechanics in Design-Structural Joints, Cape Cod, Massachusetts, Sept. 10-12, 1974.

14. Lager, John R.; and June, Reid R.: Compressive Strength of Boron-Epoxy Composites. Journal of Composite Materials, Vol. 3, January 1969, pp. 48-56.

15. Giles, Gary L.; Blackburn, Charles L.: Procedure For Efficiently Generating, Checking, and Displaying NASTRAN Input and Output Data For Analysis of Aerospace Vehicle Structures. NASTRAN: Users' Experiences, NASA TMX-2378, 1971.